Downloaded from https://academic.oup.com/mnras/article/497/2/1966/5873676 by Syracuse University College of Law user on 28 October 2020

MNRAS 497, 1966–1971 (2020) Advance Access publication 2020 July 20

# Measuring the eccentricity of GW170817 and GW190425

Amber K. Lenon <sup>10</sup>, <sup>1★</sup> Alexander H. Nitz <sup>102,3</sup> and Duncan A. Brown <sup>101,4</sup>

Accepted 2020 July 16. Received 2020 July 15; in original form 2020 June 2

#### ABSTRACT

Two binary neutron star mergers, GW170817 and GW190425, have been detected by Advanced LIGO and Virgo. These signals were detected by matched-filter searches that assume that the star's orbit has circularized by the time their gravitational-wave emission is observable. This suggests that their eccentricity is low, but full parameter estimation of their eccentricity has not yet been performed. We use gravitational-wave observations to measure the eccentricity of GW170817 and GW190425. We find that the eccentricity at a gravitational-wave frequency of 10 Hz is e < 0.024 and e < 0.048 for GW170817 and GW190425, respectively (90 per cent confidence). This is consistent with the binaries being formed in the field, as such systems are expected to have circularized to  $e \le 10^{-4}$  by the time they reach the LIGO-Virgo band. Our constraint is a factor of 2 smaller that an estimate based on GW170817 being detected by searches that neglect eccentricity. However, we caution that we find significant prior dependence in our limits, suggesting that there is limited information in the signals. We note that other techniques used to constrain binary neutron star eccentricity without full parameter estimation may miss degeneracies in the waveform, and that for future signals, it will be important to perform full parameter estimation with accurate waveform templates.

**Key words:** gravitational waves – stars: neutron – binaries: general.

### 1 INTRODUCTION

The Advanced LIGO and Virgo observatories have detected two binary neutron star mergers, GW170817 (Abbott et al. 2017c) and GW190425 (Abbott et al. 2020c). To date, 17 double neutron star systems have been observed through radio surveys of the Milky Way field (Martinez et al. 2017; Tauris et al. 2017; Cameron et al. 2018; Lynch et al. 2018; Stovall et al. 2018). Observations of binary neutron stars allow us to determine their formation channels (Smarr & Blandford 1976; Canal, Isern & Labay 1990; Portegies Zwart & Yungelson 1998; Postnov & Yungelson 2006; Kalogera et al. 2007; Kowalska et al. 2011; Beniamini & Piran 2016; Palmese et al. 2017; Tauris et al. 2017; Belczynski et al. 2018; Giacobbo & Mapelli 2018; Mapelli & Giacobbo 2018; Vigna-Gómez et al. 2018; Andrews & Mandel 2019), constrain the neutron-matter equation of state (Bauswein et al. 2017; Abbott et al. 2018; Annala et al. 2018; De et al. 2018; Fattoyev, Piekarewicz & Horowitz 2018; Most et al. 2018; Tews, Margueron & Reddy 2018; Coughlin et al. 2019; Forbes et al. 2019; Radice & Dai 2019; Capano et al. 2020), and test the strong-field regime of general relativity (Abbott et al. 2019).

Although the eccentricity of double neutron stars in the Milky Way field ranges from 0.06 to 0.828 (Zhu et al. 2018; Andrews & Mandel 2019), field binaries will circularize to eccentricity  $e < 10^{-4}$  (Peters 1964; Kowalska et al. 2011), making them detectable by matchedfilter searches that neglect eccentricity (Martel & Poisson 1999; Cokelaer & Pathak 2009; Brown & Zimmerman 2010; Huerta &

Brown 2013). GW170817 and GW190425 were detected by searches that neglect eccentricity (Abbott et al. 2017c, 2020c), suggesting that their eccentricity is  $e \lesssim 0.05$  (Huerta & Brown 2013); however, no full parameter estimation of their eccentricity has been performed. The eccentricity of binary black hole observations (Abbott et al. 2016a, b, 2017a, b, d, 2020a) has been explored in Romero-Shaw, Lasky & Thrane (2019) and Wu, Cao & Zhu (2020). Romero-Shaw et al. (2020) place a limit on the eccentricity of GW190425 by estimating the effect of eccentricity on the measured parameters of the signal. Here, we directly measure the eccentricity of GW170817 and GW190425 using Bayesian parameter estimation (Biwer et al. 2019).

We use the observations from the Gravitational-Wave Open Science Center (Abbott et al. 2017c, 2020c), waveform templates that include eccentricity (Moore et al. 2016), and Markov Chain Monte Carlo (MCMC) parameter estimation (Foreman-Mackey et al. 2013; Biwer et al. 2019) to measure the eccentricity of the GW170817 and GW190425 when they have a gravitational-wave frequency of 10 Hz. We find that the eccentricity of GW170817 is  $e \le 0.024$  and GW190425 is  $e \le 0.048$  at 90 per cent confidence for a uniform prior on e. Our limit on eccentricity of GW170817 is a factor of 2 smaller than the limit estimated by its detection with circular waveform templates. We note that when using a common prior on eccentricity, our limit on the eccentricity of GW190425 is a factor of 3 greater than the limit of Romero-Shaw et al. (2020). This is due to a degeneracy between the chirp mass and eccentricity that is not included in the analysis of Romero-Shaw et al. (2020). However, this difference does not invalidate their conclusions about the formation

<sup>&</sup>lt;sup>1</sup>Department of Physics, Syracuse University, Syracuse NY 13244, USA

<sup>&</sup>lt;sup>2</sup>Max-Planck-Institut für Gravitationsphysik (Albert-Einstein-Institut), D-30167 Hannover, Germany

<sup>&</sup>lt;sup>3</sup>Leibniz Universität Hannover, D-30167 Hannover, Germany

<sup>&</sup>lt;sup>4</sup>Kavli Institute for Theoretical Physics, University of California, Santa Barbara, CA 93106, USA

<sup>\*</sup> E-mail: alenon@syr.edu

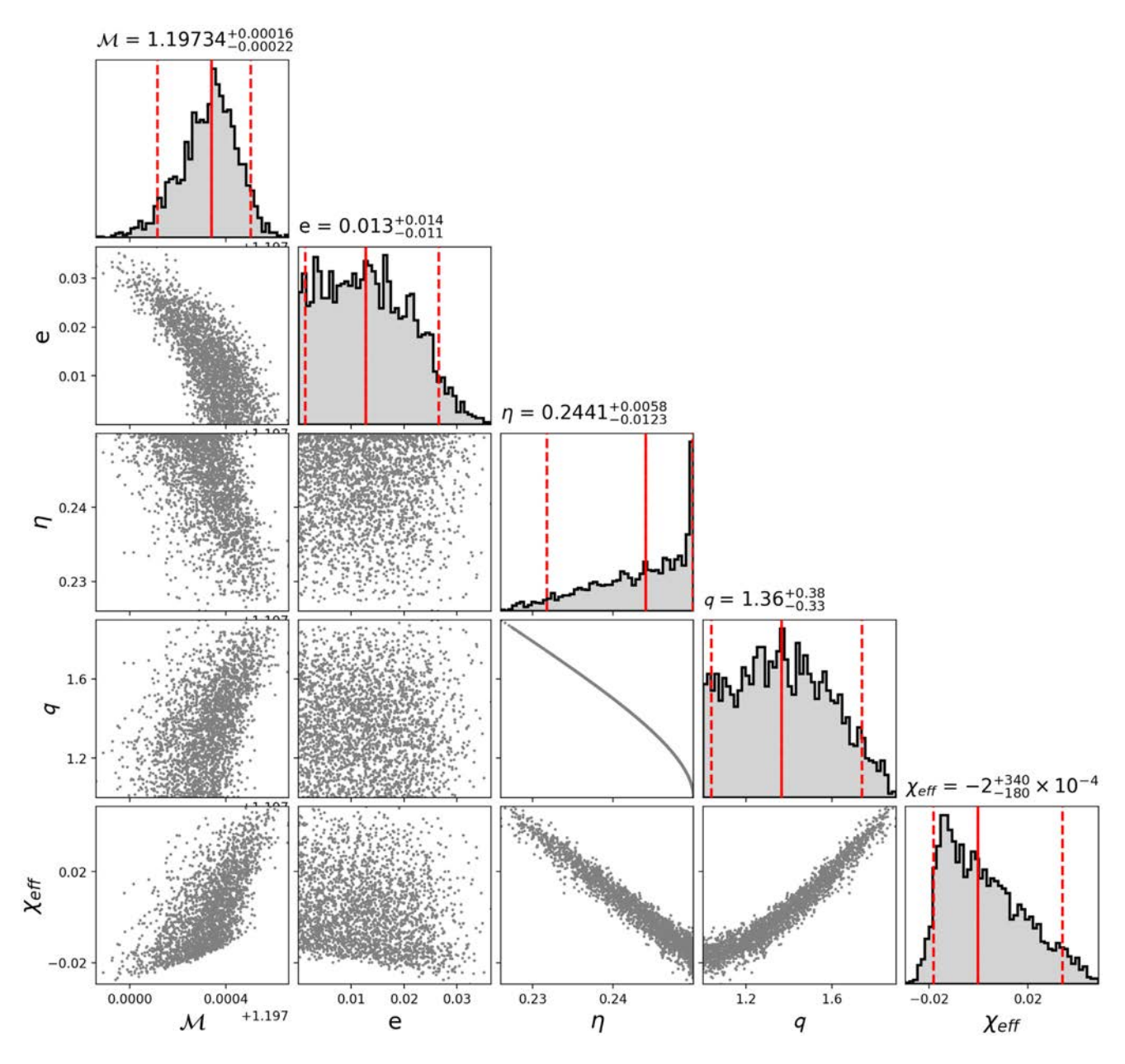


Figure 1. Posterior probability distribution of GW170817 at 10 Hz. The analysis used a prior uniform in e. Each parameter is quoted with a median value (solid red line) and a 90 per cent credible interval (dashed red lines). The chirp mass  $\mathcal{M}$  is given in the detector frame. Note the degeneracy between  $\mathcal{M}$  and e.

of GW190425. When considering the two priors we use in our analysis, the limit on the eccentricity of GW190425 changes by a factor of 2, suggesting that the eccentricity-constraining information in the signal is limited.

Dynamical interactions may form binary neutron stars with residual eccentricity, although the rate of such mergers is expected to be small in current detectors (Lee, Ramirez-Ruiz & van de Ven 2010; Ye et al. 2020), and a search for eccentric binary neutron stars in the O1 and O2 observing runs did not yield any candidates (Nitz, Lenon & Brown 2019). However, since eccentricity is an interesting probe of binary formation channels and eccentric binaries may produce different electromagnetic emission than circular binary neutron stars (Radice et al. 2016; Chaurasia et al. 2018), it is important to accurately constrain the eccentricity of binary neutron

stars as the number of observed mergers increases in the coming years.

#### 2 METHODS

We measure the parameters of GW170817 and GW190425 using Bayseian inference (Finn 2001; Rover, Meyer & Christensen 2006). We use gravitational-wave data from Advanced LIGO and Virgo (Blackburn et al. 2017; Abbott et al. 2020b),  $\boldsymbol{d}(t)$ , and a model of the gravitational waves,  $\boldsymbol{H}$ , to calculate the posterior probability density function,  $p(\boldsymbol{\theta}|\boldsymbol{d}(t), \boldsymbol{H})$ , given by

$$p(\boldsymbol{\theta}|\boldsymbol{d}(t),H) = \frac{p(\boldsymbol{\theta}|H)p(\boldsymbol{d}(t)|\boldsymbol{\theta},H)}{p(\boldsymbol{d}(t)|H)},$$
(1)

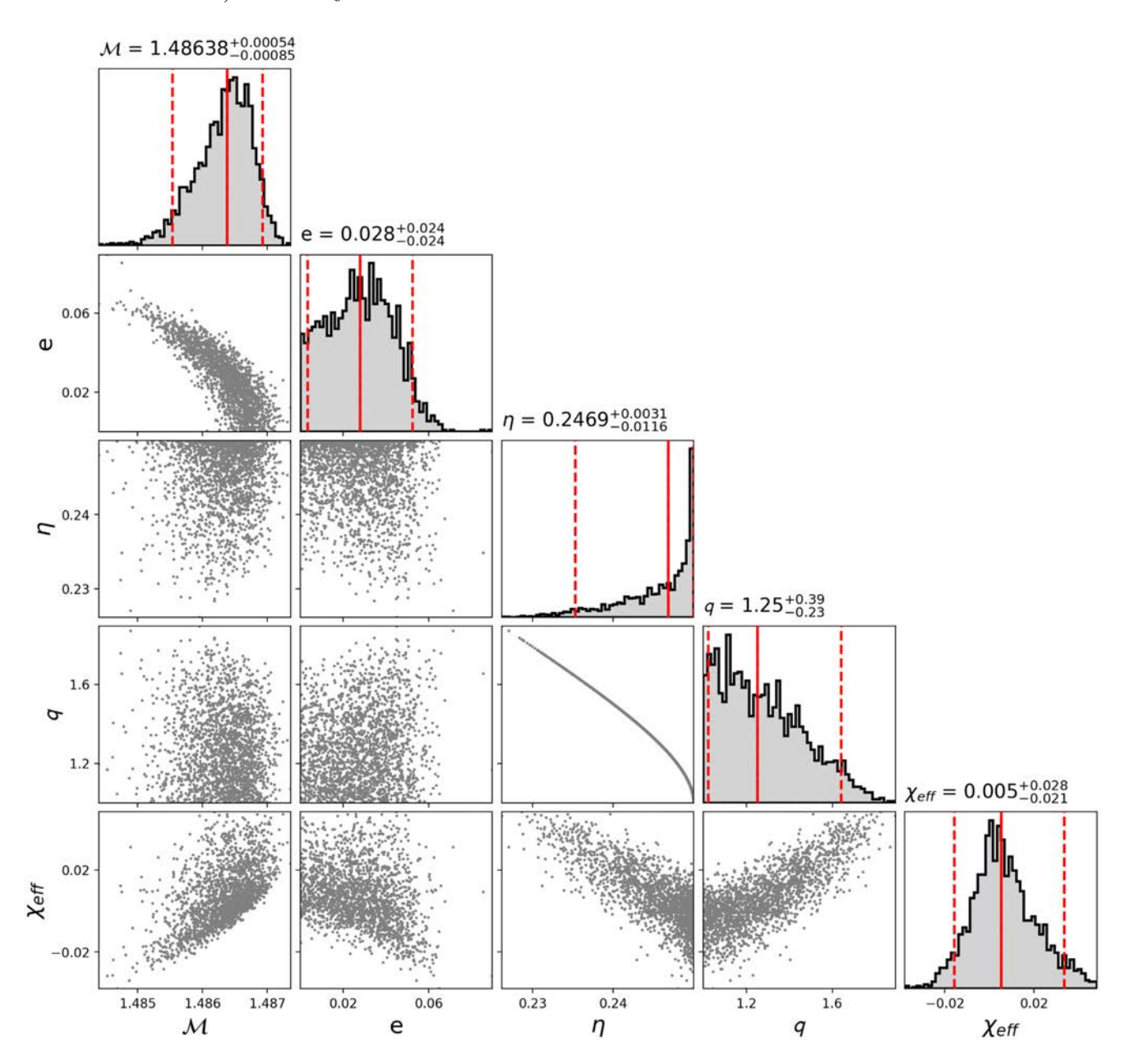


Figure 2. Posterior probability distribution of GW190425 at 10 Hz. The analysis used a prior uniform in e. Each parameter is quoted with a median value (solid red line) and a 90 per cent credible interval (dashed red lines). The chirp mass  $\mathcal{M}$  is given in the detector frame. Note the degeneracy between  $\mathcal{M}$  and e.

where  $\theta$  denotes the parameters of the gravitational waveform,  $p(\theta|H)$ , is the prior distribution on the signal parameters, and  $p(d(t)|\theta,H)$ , is the probability of observing the data, known as the likelihood. The likelihood models the noise in the detector as a Gaussian and depends upon a noise-weighted inner product between the gravitational waveform and gravitational-wave data, d(t). MCMC techniques can be used to marginalize over the parameters to obtain the posterior probabilities (Christensen & Meyer 2001). Our implementation of Bayesian inferences uses the *PyCBC Inference* software package (Biwer et al. 2019; Nitz et al. 2020) and the parallel-tempered EMCEE sampler, emcee\_pt (Foreman-Mackey et al. 2013; Vousden, Farr & Mandel 2016).

For GW170817 and GW190425, the MCMC is performed over the component masses of the binary,  $m_{1,2}$ , the component spins aligned with the orbital angular momentum,  $\chi_{1,2}$ , the time of coalescence,

 $t_{\rm c}$ , the polarization of the GW,  $\psi$ , the inclination angle,  $\iota$ , and the eccentricity, e.

We assume a uniform prior distribution on the component masses, component spins, and coalescence time around the trigger shown in Table 1. We assume an isotropic sky location for GW190425 and a prior uniform in  $\sin \iota$  for the inclination angle of both detections. We fix the sky location of GW170817 to the observed EM counterpart using a Gaussian prior distribution on the distance (Cantiello et al. 2018). We explore the prior distribution on the eccentricity by running the MCMC with two prior distributions: a prior that is uniform in e and a prior uniform in  $\log e$  to compare with the GW190425 results found by Romero-Shaw et al. (2020).

We use the GW strain data from the Advanced LIGO and Virgo detectors for GW170817 and GW190425, available through the LIGO Open Science Center (LOSC) (Vallisneri et al. 2015).

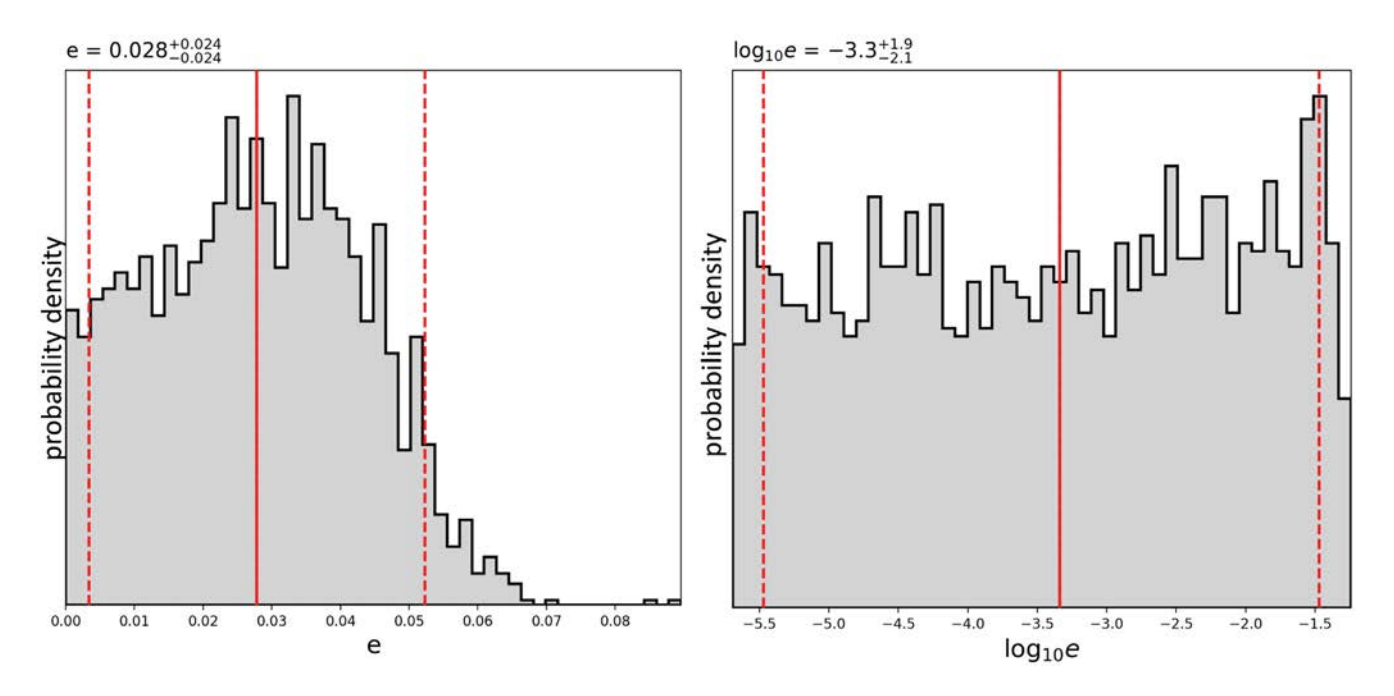


Figure 3. Eccentricity posteriors of GW190425 (solid black line) plotted for two choices of prior: uniform in e (left) and uniform in  $\log_{10}(e)$  (right). We quote the median (solid red line) and 90 per cent credible interval (dashed red lines) for e in each posterior.

Table 1. Prior distributions and GPS time intervals for GW170817 and GW190425.

Parameters	GW170817	GW190425
Component masses M <sub>☉</sub>	(1.0,3.0)	(1.0,3.0)
Component spins	(-0.05, 0.05)	(-0.05, 0.05)
Coalescence time (s)	(1187008882.33,1187008882.53)	
		(1240215502.917,1240215503.117)
Polarization	$(0,2\pi)$	$(0,2\pi)$
Inclination angle	$\sin\iota$	$\sin\iota$
Distance (Mpc)	$40.7 \pm 2.36$ (Cantiello et al. 2018)	Uniform in comoving volume
RA/Dec (°)	3.44615914, -0.40808407 (Soares-Santos et al.	$(-\pi/2, \pi/2)$
	2017)	
Eccentricity	(0.0,0.1)	(0.0,0.1)
PSD estimation interval (s)	(1187008382,1187008918)	(1240215003,1240215543)
Likelihood interval (s)	(1187008692,1187008892)	(1240215313,1240215513)

The LOSC\_CLN\_4\_V1 data that we use for GW170817 include post-processing noise subtraction performed by the LIGO/Virgo Collaboration (Blackburn et al. 2017; Driggers et al. 2019). The T1700406\_v3 data that we use for GW190425 include preprocessing glitch removal performed by the LIGO/Virgo Collaboration specifically for use in parameter estimation (Abbott et al. 2020b, c).

We high-pass the data using an eighth-order Butterworth filter with an attenuation of 0.1 at 15 Hz. To conserve the phase of the delay, the filter is applied forward and backwards. A low-pass finite impulse response filter is applied to the data prior to resampling. The data are decimated to 2048 Hz for the analysis. For computing the likelihood, we use Welch's method to estimate the detector's noise power spectral density (PSD). Welch's method is used with 16-s Hanning windowed segments that are overlapped by 8 s. The PSD is shortened to 8 s in the time domain (Allen et al. 2012). The gravitational-wave data, d(t), used in the likelihood are taken from the intervals shown in Table 1. The gravitational-wave likelihood is evaluated from a low-frequency cutoff of 20 Hz to the Nyquist frequency of 1024 Hz.

A variety of waveforms are available that model eccentricity (Huerta et al. 2014; Moore et al. 2016; Tanay, Haney & Gopakumar 2016; Cao & Han 2017; Huerta et al. 2017; Hinder, Kidder & Pfeiffer 2018; Moore & Yunes 2019; Tiwari et al. 2019). From what we know of binary neutron star mergers, we expect them to have low mass, spin, and eccentricity, making TaylorF2Ecc a suitable waveform. The waveform model, H, is TaylorF2Ecc, a TaylorF2 post-Newtonian (pN) model with eccentric corrections. We use the LIGO Algorithm Library implementation (LIGO Scientific Collaboration 2018) accurate to 3.5 pN order in orbital phase (Buonanno et al. 2009); 3.5 pN order in the spin-orbit interactions (Bohé, Marsat & Blanchet 2013); 2.0 pN order in spin-spin, quadrupole-monopole, and self-interactions of individual spins (Mikoczi, Vasuth & Gergely 2005; Arun et al. 2009); and 3.0 pN order in eccentricity (Moore et al. 2016). Since TaylorF2Ecc follows TaylorF2 in its construction, the waveform will terminate at twice the orbital frequency of a particle at the innermost stable circular orbit of a Schwarzschild black hole.

As a check on our analysis, we estimate the parameters of GW170817 and GW190425 using two available waveforms: the

TaylorF2Ecc waveform at e=0 and the TaylorF2 waveform. Our analyses are consistent with each other and with the parameters estimated by Advanced LIGO and Virgo (Abbott et al. 2017c, 2020c).

#### 3 RESULTS

We first constrain the level of the eccentricity by using the TaylorF2Ecc waveform and a prior uniform in e. We find that the 90 per cent credible intervals at  $10\,\mathrm{Hz}$  for GW170817 and GW190425 are  $e=0.012^{+0.013}_{-0.012}$  and  $e=0.025^{+0.022}_{-0.025}$ , respectively. A degeneracy between the chirp mass,  $\mathcal{M}$ , and eccentricity, e, and a small correlation between the effective spin,  $\chi_{\rm eff}$ , and e are shown in our posterior distributions in Figs 1 and 2. Since  $\mathcal{M}$  and  $\chi_{\rm eff}$  are correlated (Baird et al. 2013; Safarzadeh, Farr & Ramirez-Ruiz 2020), this will create a small correlation between e and  $\chi_{\rm eff}$ .

Romero-Shaw et al. (2020) estimated the eccentricity of GW190425 to determine if the formation channel was due to unstable BB mass transfer. They estimate the eccentricity induced by the supernova kick in this formation scenario to be between  $10^{-6}$  and  $10^{-3}$  at 10 Hz. To measure the eccentricity of GW190425, Romero-Shaw et al. (2020) reweight the posterior samples from the parameter estimation performed using circular binaries to estimate the limit of the eccentricity using the same method used to estimate the eccentricity of binary black holes (Romero-Shaw et al. 2019). They estimate the eccentricity of GW190425 at 10 Hz to be  $e \le 0.007$  (90 per cent confidence) using a prior uniform in  $\log e$ . They find no evidence for or against unstable BB mass transfer as their analysis is not able to distinguish the small residual eccentricity expected from the investigated formation channel.

To more directly compare our limit on GW190425's eccentricity, we repeat our analysis using a  $\log e$  prior. In Fig. 3, we can see the differences in the posterior distributions of each prior. With the  $\log e$  prior, we estimate the eccentricity at 10 Hz to be e < 0.023. This is a factor of 3 larger than interval estimated by Romero-Shaw et al. (2020). By re-weighting the posterior samples rather than a full MCMC, the degeneracy between  $\mathcal{M}$  and e is missed. We find that by excluding posterior samples with lower values of  $\mathcal{M}$ , we can recover the upper limit reported by Romero-Shaw et al. (2020). Although our limit on the eccentricity is larger than that of Romero-Shaw et al. (2020), our result does not change their conclusion: indeed, the strong dependence of the eccentricity posterior on the prior seen in Fig. 3 agrees with their conclusion that the signalto-noise ratio of GW190425 is not large enough to explore the eccentricities expected in BB mass transfer. We would need to be able to determine the eccentricity at lower frequencies to distinguish the formation channel.

# 4 CONCLUSION

Our analysis used the gravitational-wave observations as well as a prior on the eccentricity to constrain the eccentricity of GW170817 and GW190425. Our 90 per cent confidence limit, using a uniform prior on e for GW170817,  $e \le 0.024$ , and GW190425,  $e \le 0.048$ , is consistent with expectations since they were found by a circular search (Peters 1964). We have constrained the eccentricity to a factor of 2 smaller than estimates obtained from circular searches (Brown & Zimmerman 2010; Huerta & Brown 2013). Our 90 per cent credible intervals on the eccentricity of GW190425 are approximately a factor of 6 larger than the interval estimated by Romero-Shaw et al. (2020), which used a prior uniform in  $\log e$ . This demonstrates the impact of prior choice and the importance of measuring the eccentricity of

signals using full parameter estimation to account for the correlation between parameters.

Unfortunately, based on current merger rate estimates, the detection of an eccentric binary neutron star merger will be difficult with current observatories (Lee et al. 2010; Nitz et al. 2019; Ye et al. 2020), but gravitational waves capture binaries that have  $e \geq 0.8$  and could form in the LIGO–Virgo band (Rodriguez et al. 2018; Takátsy, Bécsy & Raffai 2019). However, since the eccentricity of the detections is expected to be low and negligible,  $e \leq 0.02$ , a circular search is effective in detecting them (Brown & Zimmerman 2010; Huerta & Brown 2013). The detection of binary neutron star mergers with high eccentricity or spin in future observing runs or with thirdgeneration detectors (Reitze et al. 2019; Maggiore et al. 2020) will reveal more about the formation channel of eccentric binaries and the existence of a dynamical formation channel.

#### **ACKNOWLEDGEMENTS**

We acknowledge the Max Planck Gesellschaft for support and the Atlas cluster computing team at the Albert-Einstein-Institut in Hannover. This research was supported in part by the National Science Foundation under grant no. PHY-1748958. Duncan Brown thanks National Science Foundation grant no. PHY-1707954 for support. Amber Lenon thanks National Science Foundation grant no. AST-1559694 for support. This research has made use of data, software, and/or web tools obtained from the Gravitational Wave Open Science Center (https://www.gw-openscience.org), a service of LIGO Laboratory, the LIGO Scientific Collaboration, and the Virgo Collaboration. LIGO is funded by the U.S. National Science Foundation. Virgo is funded by the French Centre National de Recherche Scientifique (CNRS), the Italian Istituto Nazionale della Fisica Nucleare (INFN), and the Dutch Nikhef, with contributions by Polish and Hungarian institutes.

#### DATA AVAILABILITY

The data underlying this article are available in the associated data release on GitHub, at https://github.com/gwastro/bns-eccentric-pe (Lenon, Nitz & Brown 2020).

## REFERENCES

Abbott B. et al., 2016a, Phys. Rev. Lett., 116, 061102
Abbott B. P. et al., 2016b, Phys. Rev. Lett., 116, 241103
Abbott B. P. et al., 2017a, Phys. Rev. Lett., 118, 221101
Abbott B. et al., 2017b, Phys. Rev. Lett., 119, 141101
Abbott B. P. et al., 2017c, Phys. Rev. Lett., 119, 161101
Abbott B. P. et al., 2017d, ApJ, 851, L35
Abbott B. et al., 2018, Phys. Rev. Lett., 121, 161101
Abbott B. et al., 2019, Phys. Rev. Lett., 123, 011102
Abbott B. et al., 2020a, preprint()
Abbott B. P. et al., 2020b, Glitch model for gw190425.
Abbott B. et al., 2020c, ApJ, 892, L3

Allen B., Anderson W. G., Brady P. R., Brown D. A., Creighton J. D. E., 2012, Phys. Rev. D, 85, 122006

Andrews J. J., Mandel I., 2019, ApJ, 880, L8

Annala E., Gorda T., Kurkela A., Vuorinen A., 2018, Phys. Rev. Lett., 120, 172703

Arun K. G., Buonanno A., Faye G., Ochsner E., 2009, Phys. Rev. D, 79, 104023

Baird E., Fairhurst S., Hannam M., Murphy P., 2013, Phys. Rev. D, 87, 024035 Bauswein A., Just O., Janka H.-T., Stergioulas N., 2017, ApJ, 850, L34 Belczynski K. et al., 2018, preprint(arXiv:e-print) Beniamini P., Piran T., 2016, MNRAS, 456, 4089 Biwer C. M., Capano C. D., De S., Cabero M., Brown D. A., Nitz A. H., Raymond V., 2019, PASA, 131, 024503

Blackburn K., Weinstein A., Kanner J., Chassande-Mottin E., 2017, Losc cln data products for gw170817.

Bohé A., Marsat S., Blanchet L., 2013, Class. Quant. Grav., 30, 135009

Brown D. A., Zimmerman P. J., 2010, Phys. Rev. D, 81, 024007

Buonanno A., Iyer B., Ochsner E., Pan Y., Sathyaprakash B. S., 2009, Phys. Rev. D, 80, 084043

Cameron A. et al., 2018, MNRAS, 475, L57

Canal R., Isern J., Labay J., 1990, ARA&A, 28, 183

Cantiello M. et al., 2018, ApJ, 854, L31

Cao Z., Han W.-B., 2017, Phys. Rev. D, 96, 044028

Capano C. D. et al., 2020, Nature Astron., 4, 625

Chaurasia S. V., Dietrich T., Johnson-McDaniel N. K., Ujevic M., Tichy W., Brügmann B., 2018, Phys. Rev. D, 98, 104005

Christensen N., Meyer R., 2001, Phys. Rev. D, 64, 022001

Cokelaer T., Pathak D., 2009, Class. Quant. Grav., 26, 045013

Coughlin M. W., Dietrich T., Margalit B., Metzger B. D., 2019, MNRAS, 489, L91

De S., Finstad D., Lattimer J. M., Brown D. A., Berger E., Biwer C. M., 2018, Phys. Rev. Lett., 121, 091102

Driggers J. C. et al., 2019, Phys. Rev. D, 99, 042001

Fattoyev F., Piekarewicz J., Horowitz C., 2018, Phys. Rev. Lett., 120, 172702 Finn L. S., 2001, Phys. Rev. D, 63, 102001

Forbes M. M., Bose S., Reddy S., Zhou D., Mukherjee A., De S., 2019, Phys. Rev. D, 100, 083010

Foreman-Mackey D., Hogg D. W., Lang D., Goodman J., 2013, PASA, 125, 306

Giacobbo N., Mapelli M., 2018, MNRAS, 480, 2011

Hinder I., Kidder L. E., Pfeiffer H. P., 2018, Phys. Rev. D, 98, 044015

Huerta E. A., Brown D. A., 2013, Phys. Rev. D, 87, 127501

Huerta E. A., Kumar P., McWilliams S. T., O'Shaughnessy R., Yunes N., 2014, Phys. Rev. D, 90, 084016

Huerta E. et al., 2017, Phys. Rev. D, 95, 024038

Kalogera V., Belczynski K., Kim C., O'Shaughnessy R. W., Willems B., 2007, Phys. Rept., 442, 75

Kowalska I., Bulik T., Belczynski K., Dominik M., Gondek-Rosinska D., 2011, A&A, 527, A70

Lee W. H., Ramirez-Ruiz E., van de Ven G., 2010, ApJ, 720, 953

Lenon A. K., Nitz A. H., Brown D. A., 2020, Data Release: Measuring the Eccentricity of GW170817 and GW190425. https://github.com/gwastro/bns-eccentric-pe

LIGO Scientific Collaboration, 2018, LIGO Algorithm Library - LALSuite. free software (GPL).

Lynch R. S. et al., 2018, ApJ, 859, 93

Maggiore M. et al., 2020, JCAP, 03, 050

Mapelli M., Giacobbo N., 2018, MNRAS, 479, 4391

Martel K., Poisson E., 1999, Phys. Rev. D, 60, 124008

Martinez J. et al., 2017, ApJ, 851, L29

Mikoczi B., Vasuth M., Gergely L. A., 2005, Phys. Rev. D, 71, 124043

Moore B., Yunes N., 2019, Class. Quant. Grav., 36, 185003

Moore B., Favata M., Arun K. G., Mishra C. K., 2016, Phys. Rev. D, 93, 124061

Most E. R., Weih L. R., Rezzolla L., Schaffner-Bielich J., 2018, Phys. Rev. Lett., 120, 261103

Nitz A. H., Lenon A., Brown D. A., 2019, ApJ, 890, 1

Nitz A. et al., 2020, gwastro/pycbc: Pycbc release v1.15.4.

Palmese A. et al., 2017, ApJ, 849, L34

Peters P. C., 1964, Phys. Rev., 136, B1224

Portegies Zwart S. F., Yungelson L. R., 1998, A&A, 332, 173

Postnov K., Yungelson L., 2006, Living Rev. Rel., 9, 6

Radice D., Dai L., 2019, Eur. Phys. J. A, 55, 50

Radice D., Galeazzi F., Lippuner J., Roberts L. F., Ott C. D., Rezzolla L., 2016, MNRAS, 460, 3255

Reitze D. et al., 2019, Bull. Am. Astron. Soc., 51, 035

Rodriguez C. L., Amaro-Seoane P., Chatterjee S., Kremer K., Rasio F. A., Samsing J., Ye C. S., Zevin M., 2018, Phys. Rev. D, 98, 123005

Romero-Shaw I. M., Lasky P. D., Thrane E., 2019, MNRAS, 490, 5210

Romero-Shaw I. M., , , Farrow N., Stevenson S., Thrane E., Zhu X.-J., 2020, MNRASL, 496, L64

Rover C., Meyer R., Christensen N., 2006, Class. Quant. Grav., 23, 4895 Safarzadeh M., Farr W. M., Ramirez-Ruiz E., 2020, ApJ, 894, 129

Smarr L. L., Blandford R., 1976, ApJ, 207, 574

Soares-Santos M. et al., 2017, ApJ, 848, L16

Stovall K. et al., 2018, ApJ, 854, L22

Takátsy J., Bécsy B., Raffai P., 2019, MNRAS, 486, 570

Tanay S., Haney M., Gopakumar A., 2016, Phys. Rev. D, 93, 064031

Tauris T. et al., 2017, ApJ, 846, 170

Tews I., Margueron J., Reddy S., 2018, Phys. Rev. C, 98, 045804

Tiwari S., Achamveedu G., Haney M., Hemantakumar P., 2019, Phys. Rev. D, 99, 124008

Vallisneri M., Kanner J., Williams R., Weinstein A., Stephens B., 2015, J. Phys. Conf. Ser., 610, 012021

Vigna-Gómez A. et al., 2018, MNRAS, 481, 4009

Vousden W. D., Farr W. M., Mandel I., 2016, MNRAS, 455, 1919

Wu S., Cao Z., Zhu Z.-H., 2020, MNRAS, 495, 466

Ye C. S., Fong W.-f., Kremer K., Rodriguez C. L., Chatterjee S., Fragione G., Rasio F. A., 2020, ApJ, 888, L10

Zhu X., Thrane E., Oslowski S., Levin Y., Lasky P. D., 2018, Phys. Rev. D, 98, 043002

This paper has been typeset from a TEX/LATEX file prepared by the author.